Biochemistry and Biophysics Reports 37 (2024) 101630

Contents lists available at ScienceDirect

Biochemistry and Biophysics Reports

journal homepage: www.elsevier.com/locate/bbrep

Microglia/macrophage polarization regulates spontaneous remyelination in intermittent cuprizone model of demyelination

Davood Zarini [a], Parichehr Pasbakhsh [a], Sina Mojaverrostami [a], Shiva Amirizadeh [a], Maedeh Hashemi [a], Maryam Shabani [b], Mehrazin Noshadian [a], Iraj Ragerdi Kashani [a,*]

[a] Department of Anatomy, School of Medicine, Tehran University of Medical Sciences, Tehran, Iran
[b] Department of Clinical Biochemistry, Faculty of Medicine, Tehran University of Medical Sciences, Tehran, Iran

ARTICLE INFO

Keywords:
Multiple sclerosis (MS)
Demyelination
Cuprizone
Intermittent
Glial
Macrophage

ABSTRACT

Central nervous system (CNS) lesions can repeatedly be de-and remyelinated during demyelinating diseases such as multiple sclerosis (MS). Here, we designed an intermittent demyelination model by 0.3 % Cuprizone feeding in C57/BL6 mice followed by two weeks recovery. Histochemical staining of luxol fast blue (LFB) was used for study of remyelination, detection of glial and endothelial cells was performed by immunohistochemistry staining for the following antibodies: anti Olig2 for oligodendrocyte progenitor cells, anti APC for mature oligodendrocytes, anti GFAP for astrocytes, and anti Iba-1 for microglia/macrophages, anti iNOS for M1 microglia/macrophage phenotype, anti TREM-2 for M2 microglia/macrophage phenotype and anti CD31 for endothelial cells. Also, real-time polymerase chain reaction was performed for assessment of the expression of the targeted genes. LFB staining results showed enhanced remyelination in the intermittent cuprizone (INTRCPZ) group, which was accompanied by improved motor function, increased mature oligodendrocyte cells, and reduction of astrogliosis and microgliosis. Moreover, switching from M1 to M2 polarity increased in the INTRCPZ group that was in association with downregulation of pro-inflammatory and upregulation of anti-inflammatory genes. Finally, evaluation of microvascular changes revealed a remarkable decrease in the endothelial cells in the cuprizone (CPZ) group which recovered in the INTERCPZ group. The outcomes demonstrate enhanced myelin content during recovery in the intermittent demyelination model which is in association with reshaping macrophage polarity and modification of glial and endothelial cells.

1. Introduction

Among demyelinating diseases in the central nervous system (CNS), multiple sclerosis has more incidence in young adults manifesting by multiple somatic and cognitive signs [1]. An unclear complex mechanism of glial cells interaction is involved in demyelination and remyelination events.

The area where insults occur in the CNS can be repeatedly demyelinated [2,3], however, this repeated or intermittent demyelination does not prevent remyelination [3,4]. In response to demyelinatory agents, oligodendrocyte lineage cells proliferate and migrate to the area of insult, and can differentiate into myelinating oligodendrocytes (remyelination) [5], however, it is not clear how repeated demyelination effects this mechanism.

Macrophage/microglial accumulation and astrocyte activation are seen in demyelinating diseases, including MS [6]. Microglia/macrophage are affected by the signals in their surrounding microenvironment whereby display a variety of phenotypes, including M1 polarity which is related to pro-inflammatory cytokines and M2 phenotype that promotes tissue repair by expressing anti-inflammatory factors [7]. Hypoxic condition and lower perfusion are seen in demyelinated areas [8–10]. On the other hand, M2 phenotype is involved in angiogenesis and it might overcome disease progression through improving microvasculature.

In the present study, we aimed to shed more light on the role of microglia/macrophage polarity on the microvasculature and glial cells population in the intermittent de-and remyelination model. Among several animal models of MS, cuprizone model is the best with which to investigate glial cells interaction in reaction to demyelinating events, independent of immune response and T cells. Moreover, spontaneous remyelination occurs in this model after neurotoxin withdrawal [11]. This study was designed based on intermittent cuprizone feeding to mice

* Corresponding author.
E-mail address: ragerdi@tums.ac.ir (I.R. Kashani).

https://doi.org/10.1016/j.bbrep.2023.101630
Received 28 October 2023; Received in revised form 20 December 2023; Accepted 26 December 2023

to determine brain microenvironmental changes during recovery in response to different courses of demyelination.

2. Material and methods

2.1. Study design

All animal experiments comply with the National Institutes of Health guide for the care and use of Laboratory animals (NIH Publications) and carried out in accordance with guidance from the ethical committee of Tehran University of Medical Sciences (TUMS). 30 adult male C57BL/6 mice (20–25 gr; 6–8 weeks) were purchased from Pasteur Institute of Iran (Tehran).

The mice were maintained under a normal day-night cycle (12/12) with constant temperature and humidity control and free access to food and water. For this study, the mice were randomly divided into three groups (10 mice per group), including control (Ctrl), cuprizone (CPZ), and intermittent cuprizone (INTRCPZ). The mice in the control group were fed ad libitum for 12 weeks, and mice in the CPZ group received a diet mixed with 0.3 % (w/w) cuprizone (biscyclohexanone oxaldihydrazone, Sigma Aldrich, USA) for four weeks that followed by two weeks normal diet feeding. Animals in the INTRCPZ group were fed with 0.3 % (w/w) cuprizone for four consecutive weeks and then received normal diet for two weeks aiming to summons spontaneous remyelination processes; then the mice were subsequently fed cuprizone again for another four-week demyelination run, and then received normal diet for two weeks as recovery period (Fig. 1).

2.2. Rotarod test

Three days before sacrificing the mice, they were assessed for motor behavior using a rotarod apparatus according to the manufacturer's protocol (IITC Life Science, Woodland Hills, CA, USA). Training on a slowly rotating drum one day before recording the test improves animals' skill and avoids fortuitous falling [12,13]. The test was performed for three consecutive days with three trials per day, while the interval between the trials was 15 min and gradually increasing the speed (4–40 rpm) over 5 min. The average time that a given animal stayed on the rotating drum was recorded as rotarod test time (in s).

2.3. Sacrifice and tissue preparation

At the end of each course (end of 6th and 12th weeks), anesthesia was induced in mice using intraperitoneal injection of ketamine (100 mg/kg) and xylazine (10 mg/kg). For histological assay, intracardinally perfusion was done using 0.9 % NaCl solution injection followed by 4 % Paraformaldehyde (PFA, Merck, Germany) as fixative. Brains were carefully exited, and post-fixed in 4 % PFA for 24 h. After paraffin embedding (Merck, Germany), 5 μm coronal brain sections were prepared by a microtome rotatory apparatus (Microm HM335E, Microm International GmbH, Walldorf, Germany)

2.4. Luxol fast blue staining

In order to assess the percentage of remyelination in the lateral part of the corpus callosum, which is located above the lateral ventricle (Fig. 2a), Luxol fast blue (LFB, Sigma, St. Louis, MO, USA) staining was used for randomly selected sections. According to our previous study [14], after preparing brain sections on positive charge slides, deparaffinization and rehydration were done. The slides were incubated on LFB solution (0.01 %) overnight at 56 °C (myelinated fibers appear in blue whereas demyelinated areas emerge in white). LFB-stained sections were placed under the Olympus light microscope equipped with a digital camera (Diagnostic Instruments Inc, Sterling Heights, MI, USA), and images were captured. 10 random sections were chosen from each mouse for LFB image quantification, and blue color intensity was measured using a densitometric scanning procedure (Image J Software, US National Institutes of Health, Bethesda, MD, USA). Briefly, images were converted into grayscale value (8 bit), and binary black and white pixel images were conducted after thresholding (black pixels represented the myelin) (Fig. 2b). Then, three different areas in each image were selected as Regions-Of-Interest (ROI) and were analyzed for myelin quantity by calculating pixel ratios. Finally, we calculated the percentage of myelinated areas within the ROIs by dividing the number of black pixels by total number of pixels multiplied by 100.

2.5. Quantitative real-time polymerase chain reaction (qRT-PCR)

The expression of CD86, iNOS, MRC-1, triggering receptor expressed on myeloid cell 2 (TREM-2), interleukin 1 beta (IL-1β), tumor necrosis factor (TNF)-α, TGF-β, IL-10, CD31 and VEGF-a genes in the corpus callosum was analyzed by quantitative real-time polymerase chain reaction (qRT-PCR). Anesthesia was induced in the mice by intraperitoneal injection of ketamine (100 mg/kg) and xylazine (10 mg/kg) (3 mice in each group). After decapitation, their brains were removed and immediately transferred to cold PBS which had been placed on the ice. By scratching the outer grey matter, the white border of the corpus callosum was observed, and the entire corpus callosum was separated. We immediately froze the samples in liquid nitrogen and transferred them to −80 °C freezer until used. GeneAll Hybrid-R RNA purification kit was used for total RNA isolation. After DNase treatment, assessment of RNAs' quantification, purity, and integrity were checked by a NanoDrop-1000 device (Thermo Fisher Scientific) and gel electrophoresis. cDNA was synthesized using a RevertAid First Strand cDNA Synthesis Kit (Thermo Fisher Scientific). A two-step PCR protocol was applied using SYBR Green RealQ Plus 2x Master Mix Green (Amplicon) and was run on StepOnePlus™ Real-Time PCR System. The gene expression profile was quantified using ΔCT method relative to the geometric mean (the mean of β-actin and 18-s rRNA as reference genes) and normalized with the control group. The comparison of the expression rate of target genes in different groups was presented as fold changes. The sequence of primers has been shown in Table 1.

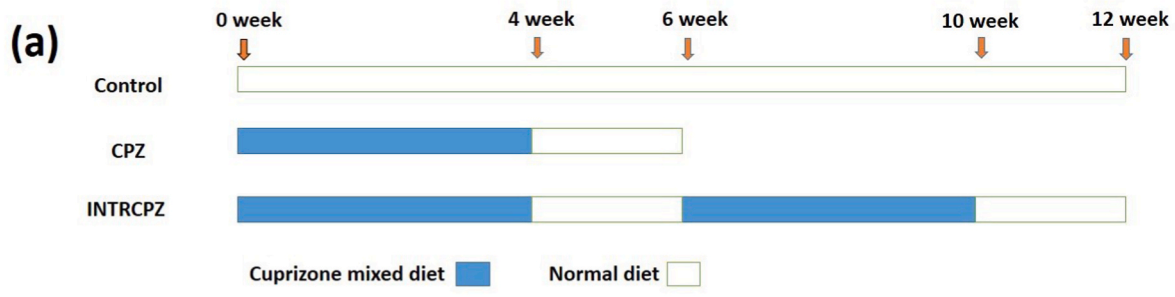

Fig. 1. Schematic representative of study design.

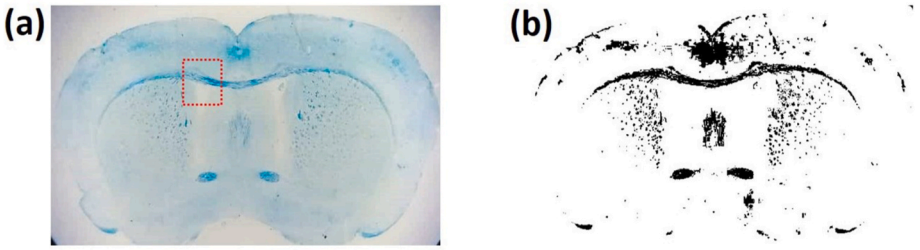

Fig. 2. **(a)** An overview image of luxol fast blue stained section and red box indicates the area of LFB and IHC study. **(b)** Grey value and thresholding for luxol fast blue quantification.

Table 1
Sequence of primers used for quantitative real-time polymerase chain reaction (qRT-PCR).

Primer name	Sequence	Primer length	Product length
Mouse β-ACTIN	Forward: CATCCGTAAAGACCTCTATGCCAAC	25	171
	Reverse: ATGGAGCCACCGATCCACA	19	
Mouse 18s rRNA	Forward: CCTGCGGCTTAATTTGACTC	20	118
	Reverse: AACTAAGAACGGCCATGCAC	20	
Mouse iNOS	Forward: TCCTACACCACACCAAAC	18	199
	Reverse: CTCCAATCTCTGCCTATCC	19	
Mouse CD86	Forward: GCACGGACTTGAACAACCAG	20	194
	Reverse: CCTTTGTAAATGGGCACGGC	20	
Mouse MRC-1	Forward: CCTCTGGTGAACGGAATGAT	19	161
	Reverse: CTTCCTTTGGTCAGCTTTGG	18	
Mouse TREM-2	Forward: ACTGGTGGAGGTGCTGGAG	19	160
	Reverse: AAGAGGAGGAAGGTGGTAGGC	21	
Mouse IL-1β	Forward: CCTTCCAGGATGAGGACATGA	22	71
	Reverse: TGAGTCACAGAGGATGGGCTC	18	
Mouse TNFα	Forward: TGCTCTGTGAAGGGAATGGG	20	142
	Reverse: ACCCTGAGCCATAATCCCCT	20	
Mouse TGFβ	Forward: ATGCTAAAGAGGTCACCCGC	20	119
	Reverse: TGCTTCCCGAATGTCTGACG	20	
Mouse IL-10	Forward: ATGCTGCCTGCTCTTACTGACTG	23	216
	Reverse: CCCAAGTAACCCTTAAAGTCCTGC	24	
Mouse CD31	Forward: GGTGCATGGCGTATCCAAG	19	173
	Reverse: TGGAGGTCTTATCTATCCTTCGC	23	
Mouse VEGF-A	Forward: ATGAACTTTCTGCTCTCTTGGGT	23	232
	Reverse: CACAGGACGGCTTGAAGATGTA	22	

2.6. Immunohistochemistry

After deparaffinization in xylene and then rehydration in descending grades of ethanol (100 %, 95 %, and 70 % ethanol), the slides were immersed in distilled water for 5 min and were boiled in 10 mM sodium citrate (pH 6.0, 20 min) for antigen retrieval. Sections were quenched by 3 % hydrogen peroxide (Merck, Darmstadt, Germany) for 10 min. In next place, 5 % bovine serum albumin (BSA) in Tris-buffered saline (TBST) was used for blocking nonspecific markers (2 h) followed by treating with primary antibodies at 4 °C: anti-APC (mature oligodendrocyte 1:250, FUJIFILM Wako Chemicals, Richmond, VA, USA), anti-Olig2 (oligodendrocyte progenitor 1:1000, Sigma, St. Louis, MO, USA), anti- Iba-1 (microglia/macrophage 1:100, FUJIFILM Wako Chemicals, Richmond, VA, USA), anti- GFAP (astrocyte 1:500, Sigma, St. Louis, MO, USA), anti-iNOS (M1 microglia/macrophage 1:500, Abcam, Cambridge, UK), anti- TREM-2 (M2 microglia/macrophage 1:1000, Sigma, St. Louis, MO, USA) and anti-CD31 (endothelial cell 1:50, Abcam, Cambridge, UK). After rinsing with TBST, HPR-conjugated secondary antibody (Vectastain® ABC kit, Vector Laboratories, Newark, CA, USA) was used for 20 min. To visualize the antigen's immunoreactivity, sections were exposed to 3,3-diaminobenzoic acid (DAB) substrate (DAKO, Waldbronn, Germany) and counterstained with hematoxylin dye. Sections were imaged under a light microscope (Olympus CX310, Tokyo, Japan) equipped with a Canon EOS digital camera and the same area which was assessed for LFB staining (Fig. 2a), was also studied for IHC staining.

2.7. Statistical analysis

GraphPad Prism (GraphPad Software, Boston, MA, USA) and SPSS software version 20 (IBM, Armonk, NY) were used for data analyzing in this experiment. Normality of data distribution was checked by Shapiro-Wilk test and comparison between three groups was done by one-way analysis of variance (ANOVA) followed by Tukey post hoc test. Data are presented as means ± SD and p-value less than 0.05 is considered statistically significant.

3. Results

3.1. The impact of intermittent demyelination on motor function and balance

Motor activity and balance were examined using rotarod test for 3 groups at 2 weeks after demyelination and intermittent demyelination induction. In comparison with the control group, cuprizone ingestion resulted in severe motor coordination deficit in one course cuprizone fed mice ($p < 0.01$), while intermittent demyelination showed lesser effect on the induction of motor balance impairment ($p < 0.05$) (Fig. 3a).

3.2. The impact of intermittent demyelination on myelin content

Staining of myelin with luxol fast blue was carried out to evaluate the amount of remyelination. Myelin content (blue color) within the corpus callosum showed a clear decrease in all cuprizone-fed mice. We used quantitative analysis for remyelination assessment within the corpus callosum, and the results showed sharp reduction of myelin content in the CPZ group (15.81 ± 0.91 %) in comparison with the control group (99.08 ± 0.25 %) ($p < 0.001$). On the other hand, there was a significant increase in the percentage of area covered by myelin in the INTRCPZ group (22.1 ± 2.05 %) compared to the CPZ group ($p < 0.05$), indicating less myelin injury two weeks after intermittent demyelination (Fig. 3b).

3.3. The impact of intermittent demyelination on mRNA expression levels of genes related to microglia/macrophage polarization and microvascular changes

To evaluate the role of intermittent demyelination in microglia/macrophage polarization and microvascular changes within the corpus callosum, RT-qPCR was used. CD86, iNOS, IL-1β and TNF-α genes were evaluated as M1 microglia/macrophage markers [15,16] and MRC-1, TREM-2, IL-10 and TGF-β genes as M2 microglia/macrophage markers [17,18].

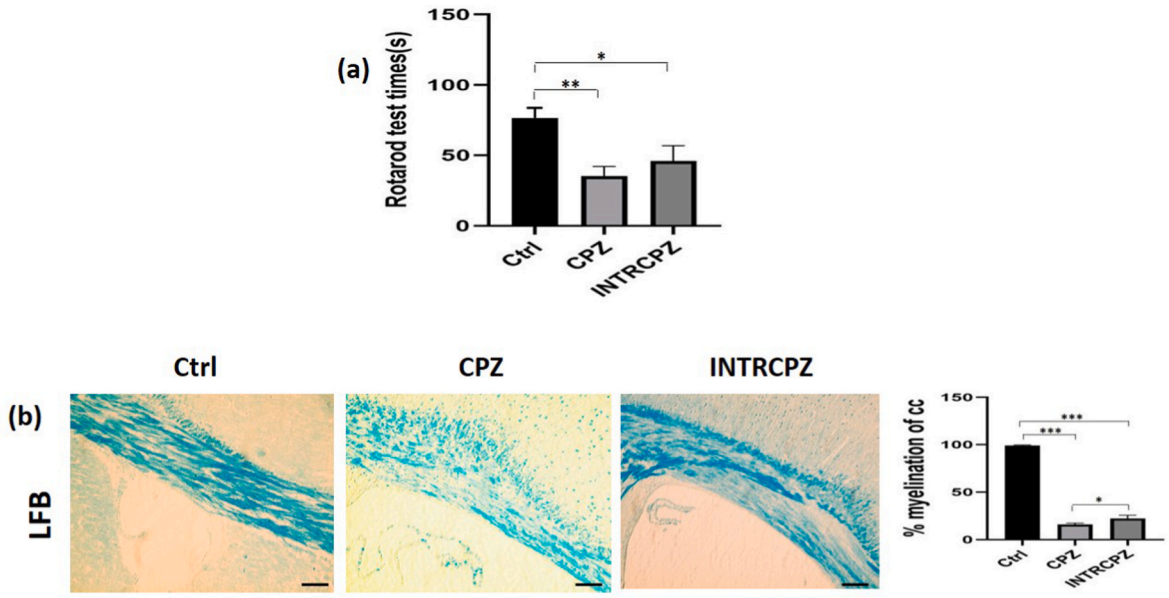

Fig. 3. **(a)** Rotarod test for evaluation of motor coordination and balance. Intermittent demyelination resulted in better performance in the INTRCPZ group. *P < 0.05, **P < 0.05 (n = 9 per group). **(b)** Luxol fast blue (LFB) for evaluation of demyelination in the corpus callosum of animals received cuprizone. The concentration of blue-stained myelinated fibers within the corpus callosum increased after intermittent demyelination, demonstrated after LFB quantification. Scale bare = 100 μm, *P < 0.05, ***$P < 0.001$.

Data analysis revealed that one course of demyelination upregulated mRNA expression of M1 microglia/macrophage markers including CD86, iNOS, IL-1β and TNF-α compared to control ($p < 0.05$ for CD86 and TNF-α, $p < 0.01$ for iNOS and IL-1β), while intermittent cuprizone feeding in the INTRCPZ group resulted in a reduced expression rate of the mRNA of iNOS and IL-1β genes compared to the CPZ group ($p < 0.05$), demonstrating decreased M1 microglia/macrophage in the intermittent cuprizone fed mice. On the other hand, when we assessed M2 microglia/macrophage markers including MRC-1, TREM-2, IL-10 and TGF-β in the CPZ group, there was a remarkable decrease in comparison with control ($p < 0.05$ for TREM-2 and IL-10, $p < 0.001$ for MRC-1, $p < 0.01$ for TGF-β), while the mice experiencing intermittent demyelination in the INTRCPZ group showed downregulation in the rate of expression of MRC-1 and TGF-β in comparison with the CPZ group (p

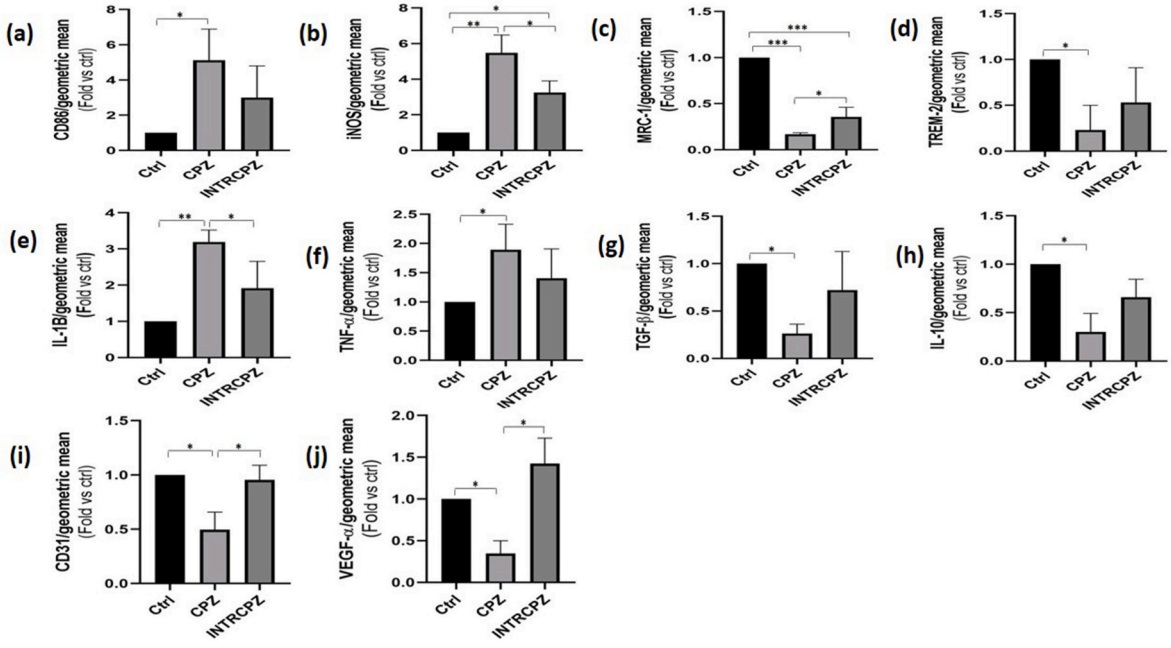

Fig. 4. Modified gene expression profile of M1/M2 polarity, pro- or anti-inflammatory cytokines in corpus callosum as the results of intermittent demyelination. (**a & b)** *CD86* and *iNOS* as specific genes related to the M1 phenotype, and (**c & d)** MRC-1 and TREM-2 as specific genes related to the M2 polarity. (**e & f)** *IL-1β* and *TNF-α* as inflammatory cytokines, (**g & h**) *TGF-β* and *IL-10* as anti-inflammatory cytokines, and **(i & g)** CD31 and VEGF-A as endothelial markers evaluated in this study. Cuprizone administration increased the mRNA level of pro-inflammatory cytokines and genes associated with the M1 cells. In contrast, expression of endothelial markers, anti-inflammatory cytokines, and genes associated with the M2 phenotype were decreased after cuprizone ingestion. The outcomes were more pronounced for animals in the CPZ group. Values were normalized to the geometric mean (18S rRNA and beta-actin). Data are shown as mean ± SEM. *$P < 0.05$, **$P < 0.01$, and ***$P < 0.001$.

< 0.05). these results revealed that a single course of cuprizone ingestion increases M1 microglia/macrophage phenotype while intermittent cuprizone feeding promotes M2 polarization.

To evaluate endothelial cells, data analysis of genes expression levels of CD31 and VEGF-A was performed and the results showed a remarkable decrease for these genes in the CPZ group as compared to control ($p < 0.05$), but intermittent cuprizone fed mice in the INTRCPZ group demonstrated a remarkable increase in the CD31 and VEGF-A expression levels compared to the CPZ group (Fig. 4).

These results obtained from RT-qPCR test revealed that increased M1 microglia/macrophage polarity after a single course of cuprizone ingestion was accompanied by diminished endothelial cells and impaired microvasculature in the CPZ group, however, intermittent cuprizone feeding increased M2 microglia/macrophage polarity and improved microvasculature in the INTRCPZ group.

3.4. Evaluation of the impact of intermittent demyelination on glial cells by immunohistochemistry staining

Myelinating oligodendrocyte and oligodendrocyte lineage cells population were evaluated within the corpus callosum using immunohistochemistry staining against APC and Olig2, respectively. The number of APC-positive cells remarkably decreased in single course cuprizone fed mice in the CPZ group (30.33 ± 3.48 cells/mm2) in comparison with the control group (375 ± 8.14 cells/mm2) ($p < 0.001$), which was accompanied by increased Olig2-positive cells in these animals (448.7 ± 18.49 cells/mm2) compared to the control group (222.7 ± 6.36 cells/mm2) ($p < 0.001$), indicating the neurotoxicity effect of cuprizone on decreasing myelinating oligodendrocyte (APC-positive) which is followed by enhancement of oligodendrocyte lineage cells (Olig2-positive) as a compensatory mechanism. However, there was a remarkable upregulation in the number of APC-positive cells and a decrease in the number of Olig2-positive cells in the INTRCPZ group (54.67 ± 6.36 cells/mm2 for APC and 389.3 ± 6.36 cells/mm2 for Olig2) compared with the CPZ group ($p < 0.05$), demonstrating an enhancement in the number of myelinating oligodendrocytes after intermittent demyelination that is resulted from differentiation of oligodendrocyte progenitor cells to myelinating oligodendrocytes.

To clarify astrogliosis and microgliosis in different groups, astrocytes and microglia were respectively assessed by GFAP and Iba-1 using immunohistochemistry staining. Importantly, single course of cuprizone intoxication resulted to a sharp increase in the frequency of GFAP and Iba-1 positive cells in the CPZ group (66.21 ± 2.01 for GFAP and 85.8 ± 4.11 for Iba-1) in comparison with the control (31.38 ± 0.41 for GFAP and 35 ± 2.61 for Iba-1) ($p < 0.001$), however, following intermittent cuprizone ingestion, the mice in the INTRCPZ group displayed a significant decrease in the area covered by astrocytes (GFAP-positive) and microglia (Iba-1positive) (58.92 ± 2.04 for GFAP and 76.78 ± 2.09 for Iba-1) compared to the CPZ group ($p < 0.05$), indicating subsided gliosis in the intermittent fed mice (Fig. 5).

3.5. Evaluation of the impact of intermittent demyelination on M1/M2 microglia/macrophage phenotype and microvascular changes by immunohistochemistry staining

Surface markers of M1, M2, and endothelial cells were respectively labeled by anti iNOS, anti TREM-2, and anti CD31 within corpus callosum using immunohistochemistry staining. We found that the number of M1 microglia/macrophage phenotype (iNOS-positive cells) were remarkably enhanced following one course of cuprizone ingestion in the CPZ group (242.7 ± 7.05 cells/mm2) in comparison with the control (45.33 ± 5.33 cells/mm2) ($p < 0.001$) that was accompanied by reduction of M2 polarization (TREM-2-positive cells) in this group (80 ± 4.61 cells/mm2) compared to control (218.7 ± 11.62 cells/mm2)) ($p < 0.01$). On the other hand, intermittent cuprizone fed mice in the INTRCPZ group displayed significant reduction in the number of iNOS-positive cells (200.7 ± 7.31 cells/mm2) compared to the CPZ group ($p < 0.05$). These data revealed that shifting from M2 to M1 phenotype

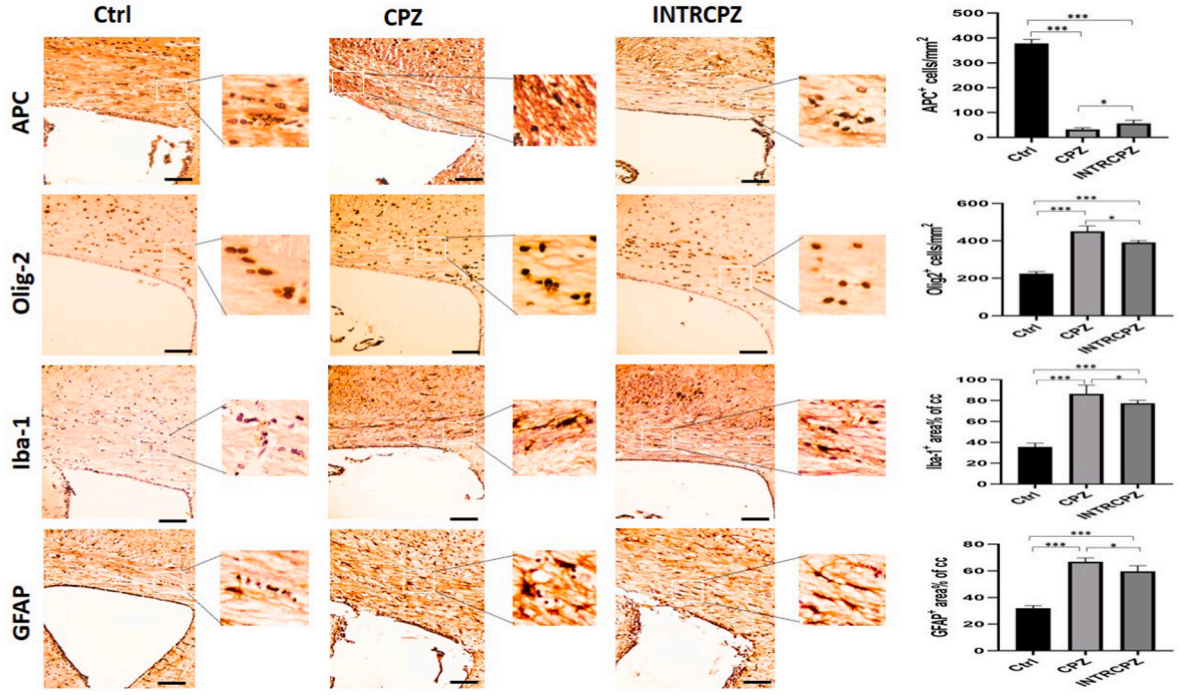

Fig. 5. Evaluation of the impact of intermittent demyelination on glial cells population in the corpus callosum by immunohistochemistry. Representative photomicrographs of mature oligodendrocyte (APC), oligodendrocyte progenitor (Olig2), astrocyte (GFAP), and microglia/macrophage (Iba1). Scale bar = 100 μm. Magnified images from the regions indicated by small white boxes are presented as large white boxes. Quantitative analysis of the immunohistochemistry results. Values are shown as mean ± SEM. *$P < 0.05$, **$P < 0.01$, and ***$P < 0.001$. APC, adenomatous polyposis coli; Olig2, oligodendrocyte transcription factor 2; GFAP, glial fibrillary acidic protein; and Iba1, ionized calcium-binding adaptor molecule 1.

occurred in a single demyelination while it can be partially compensated after intermittent demyelination.

Evaluation of the endothelial cells (CD31-positive) revealed a significant decrease in the CPZ group (2.54 ± 0.17) in comparison to the control group (3.33 ± 0.13) ($p < 0.05$), on the other hand, intermittent demyelination was followed by a remarkable increase in the CD31-positive cells in the INTRCPZ group (3.06 ± 0.13) compared to CPZ group ($p < 0.05$), indicating improved microvasculature in the intermittent cuprizone fed mice (Fig. 6).

4. Discussion

In this study, enhanced remyelination and improved motor function were accompanied by glial cells modifications, M1/M2 polarity changes and microvascular improvement in the intermittent cuprizone fed mice. Here, we used cuprizone model because spontaneous remyelination can occur after cuprizone withdrawal [19].

MS lesions may appear in the normal white matter for the first time or repeat in some lesions that experience second demyelination [2,20]. However, previous publication have recommended that remyelination can even occur after repeated demyelination in the cuprizone model [3,21]. Here we observed that intermittent demyelination increased myelin regeneration in the INTRCPZ group, whoever, it cannot be excluded that the second cuprizone administration led to less injury, as Johnson et al. reported a prolonged second demyelination period after 8 weeks recovery from the first demyelination period [3]. Also, Murta et al. reported a diminished CNS response to the second demyelinatory event if there is still an active lesion [22], as in our study, a complete remyelination has not occurred yet at the onset of the second demyelination.

Whoever, Penderis et al. demonstrated that repeated stereotaxic injection of etidium bromide does not cause retardation of the remyelination process, even extent remyelination happens after second demyelination, but they didn't explain the possible reason(s) [23]. Also, Rodriguez et al. reported that there is no difference in the myelin content after repeated demyelination [4].

Cuprizone induces oligodendrocyte-specific toxicity, which is induced by mitochondrial and metabolic dysfunction [24] and followed by subventricular zone cells proliferation, migration, and differentiation within demyelinating lesions [25]. The results of immunohistochemical staining of APCs and Olig2 revealed decreased oligodendrocytes and increased progenitors with sharp outcomes in the CPZ group. In this regard, Guglielmetti et al. and El-Akabawy et al. demonstrated that four weeks cuprizone intoxication induces severe demyelination and astrogliosis in mice [26,27].

Early microglial activation occurs during cuprizone intoxication that promotes astrocytes to produce inflammatory cytokines [28], resulted in accumulation of myelin debris as an unfavorable event in the cuprizone model [29].

Here we observed a dramatic upregulation in Iba1 and GFAP protein expression in the CPZ group, which partially compensated in the INTRCPZ group. We assumed that these glial changes might be in relation with M1/M2 phenotype and pro- or anti-inflammatory cytokines. The effect of cuprizone administration on microglia/macrophage polarization has been confirmed, and several studies have utilized different approaches to modulate microglial/macrophage activation. In this regard, it is reported that 17b-estradiol and medroxyprogesterone acetate can alter microglial polarity through reduction of NLRP3 inflammasome [30,31]. In addition, methylprednisolone acetate and metformin can switch microglia/macrophage from M1 to M2 polarity [32,33]. In our study, intermittent demyelination resulted in alteration in microglia/macrophage phenotype, so that, *CD86* and *iNOS* genes as the markers of M1 polarity were increased in the CPZ group while MRC-1 and TREM-2, which are related to M2 polarity, decreased in this group. Also, protein expression analysis of *iNOS and* TREM-2 confirmed these data, however, intermittent demyelination attenuated the outcomes in the INTRCPZ group.

M1 microglia is more specially activated in MS lesions [34] and secrets pro-inflammatory cytokines [35,36], while M2 microglia is related with Arg-1, CD206, and CX3CR1 for inhibition of neuroinflammation [15,37]. In this study, we found that increased M1 microglia was relevant to elevated pro-inflammatory cytokines of TNFα and IL-1β with a sharp outcome for the CPZ group, which was in line with previous studies [38,39]. According to the previous reports, IL-10 and TGF- β can induce M2 polarity and inhibit inflammatory cytokine production [40,

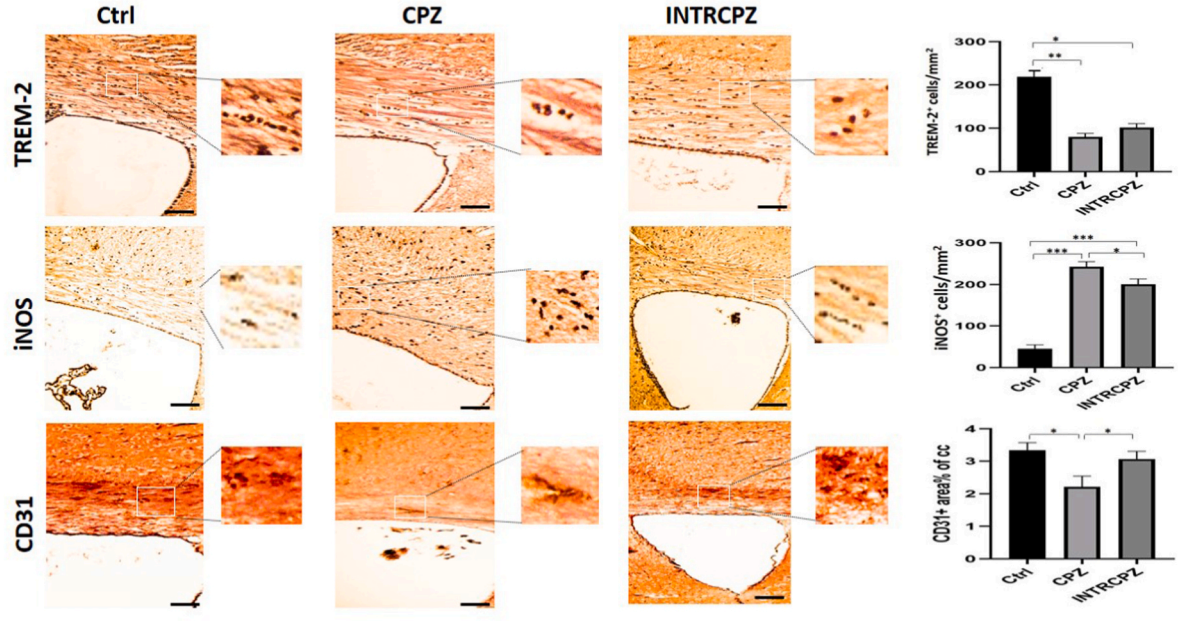

Fig. 6. Evaluation of the impact of intermittent demyelination on M1/M2 phenotype and microvascular changes in the corpus callosum by immunohistochemistry. Representative photomicrographs of M1 (iNOS), M2 (TREM-2), and endothelial (CD31) cells. Scale bar = 100 μm. Magnified images from the regions indicated by small white boxes are presented as large white boxes. Quantitative analysis of the immunohistochemistry results. Values are shown as mean ± SEM. *P < 0.05, **P < 0.01, and ***P < 0.001. iNOS, Inducible nitric oxide synthase; TREM-2, Triggering Receptor Expressed on Myeloid cells 2; CD31, Cluster of Differentiation 31.

41]. In this study, decreased M2 polarity in the CPZ group was accompanied by decreased genes expression of anti-inflammatory cytokines such as IL-10 and TGF- β in the CPZ group.

The mechanistic pathway of how remyelination increases after intermittent demyelination is no longer apparent. During cuprizone intoxication, mitochondrial dysfunction and inflammation increase energy demand in demyelinated areas that leads to an energy deficient crisis. Here, we investigated the role of angiogenesis as a compensatory response to hypoxia and energy deficiency in the intermittent cuprizone model. Hypoxia is implicated in myriad neurological disorders [42,43], and it is in close relationship with inflammation [44]. Yang and Dunn noted that reduced microvascular StO2 is likely related to hypoxic regions in MS brain [45]; more specially, numerous publications reported relatively lower perfusion in MS lesions [8,46]. In confirming these investigations, we demonstrated downregulation of CD31 and VEGF-A as the endothelial cell markers in the CPZ group, which indicates impaired microvasculature in the corpus callosum, and this is in agreement with previous works [47,48]. Cuprizone intoxication increases M1 polarity [14] but decreases microvasculature [47] which was also seen in the CPZ group in our study. Here, we showed that intermittent demyelination increased M2 microglia in the INTRCPZ group. On the other hand, according to the role of M2 polarity in increasing angiogenesis (reviewed in Ref. [49]), a raised in endothelial cell markers was observed in the INTRCPZ group which was accompanied by increased M2 polarity. Due to OPCs requirement to vasculature for migration [50], increased microvasculature in the INTRCPZ group can facilitate OPCs migration and increase remyelination after intermittent demyelination.

According to the role of M2 polarity in increasing angiogenesis [49,51], a raised angiogenesis in the INTRCPZ group was observed that was accompanied by an increased M2 phenotype in this group. Although cuprizone model is not a facsimile of multiple sclerosis, however, Rashid et al. proposed a raised perfusion in RRMS against hypoperfusion in PPMS patients [52].

Data of this study suggested a possible relation between intermittent demyelination and microvascular changes via M2 polarity mediation.

5. Conclusion

Our study has revealed that glial response to single or intermittent demyelination shows a clear difference during the recovery phase. Furthermore, microglia/macrophage polarity can influence the glial response to various demyelinating conditions.

Funding

This work was supported by Tehran University of Medical Sciences [grant number grant IR. TUMS.MEDICINE.REC.1399.237]

CRediT authorship contribution statement

Davood Zarini: Writing – review & editing, Writing – original draft, Visualization, Validation, Software, Resources, Formal analysis, Data curation, Conceptualization. **Parichehr Pasbakhsh:** Project administration, Investigation, Data curation, Conceptualization. **Sina Mojaverrostami:** Software, Methodology. **Shiva Amirizadeh:** Writing – review & editing. **Maedeh Hashemi:** Writing – original draft, Software. **Maryam Shabani:** Methodology. **Mehrazin Noshadian:** Writing – review & editing, Writing – original draft. **Iraj Ragerdi Kashani:** Visualization, Validation, Supervision, Funding acquisition, Conceptualization.

Declaration of competing interest

The authors declare that they have no known competing financial interests or personal relationships that could have appeared to influence the work reported in this paper.

Data availability

No data was used for the research described in the article.

References

[1] H. Lassmann, Multiple sclerosis pathology, Cold Spring Harbor perspectives in medicine 8 (3) (2018).
[2] R.A. Brown, S. Narayanan, D.L. Arnold, Imaging of repeated episodes of demyelination and remyelination in multiple sclerosis, Neuroimage: Clinical 6 (2014) 20–25.
[3] E.S. Johnson, S. Ludwin, The demonstration of recurrent demyelination and remyelination of axons in the central nervous system, Acta Neuropathol. 53 (1981) 93–98.
[4] E.G. Rodriguez, et al., Oligodendroglia in cortical multiple sclerosis lesions decrease with disease progression, but regenerate after repeated experimental demyelination, Acta Neuropathol. 128 (2014) 231–246.
[5] R.J. Franklin, C. Ffrench-Constant, Remyelination in the CNS: from biology to therapy, Nat. Rev. Neurosci. 9 (11) (2008) 839–855.
[6] M. Pekny, M. Nilsson, Astrocyte activation and reactive gliosis, Glia 50 (4) (2005) 427–434.
[7] R. Orihuela, C.A. McPherson, G.J. Harry, Microglial M1/M2 polarization and metabolic states, Br. J. Pharmacol. 173 (4) (2016) 649–665.
[8] M. D'haeseleer, et al., Cerebral hypoperfusion: a new pathophysiologic concept in multiple sclerosis? J. Cerebr. Blood Flow Metabol. 35 (9) (2015) 1406–1410.
[9] J. De Keyser, et al., Hypoperfusion of the cerebral white matter in multiple sclerosis: possible mechanisms and pathophysiological significance, J. Cerebr. Blood Flow Metabol. 28 (10) (2008) 1645–1651.
[10] E.M. Haacke, et al., An overview of venous abnormalities related to the development of lesions in multiple sclerosis, Front. Neurol. 12 (2021) 589.
[11] M. Kipp, et al., The cuprizone animal model: new insights into an old story, Acta Neuropathol. 118 (2009) 723–736.
[12] D.M. Samy, et al., Neurobehavioral, biochemical and histological assessment of the effects of resveratrol on cuprizone-induced demyelination in mice: role of autophagy modulation, J. Physiol. Biochem. (2023) 1–14.
[13] F. Tahmasebi, et al., The effect of microglial ablation and mesenchymal stem cell transplantation on a cuprizone-induced demyelination model, J. Cell. Physiol. 236 (5) (2021) 3552–3564.
[14] D. Zarini, et al., Protective features of calorie restriction on cuprizone-induced demyelination via modulating microglial phenotype, J. Chem. Neuroanat. 116 (2021) 102013.
[15] B.A. Durafourt, et al., Comparison of polarization properties of human adult microglia and blood-derived macrophages, Glia 60 (5) (2012) 717–727.
[16] W. Tam, C. Ma, Bipolar/rod-shaped microglia are proliferating microglia with distinct M1/M2 phenotypes, Sci. Rep. 4 (2014) 7279.
[17] J.M. Crain, M. Nikodemova, J.J. Watters, Microglia express distinct M1 and M2 phenotypic markers in the postnatal and adult central nervous system in male and female mice, J. Neurosci. Res. 91 (9) (2013) 1143–1151.
[18] K. Kobayashi, et al., Minocycline selectively inhibits M1 polarization of microglia, Cell Death Dis. 4 (3) (2013) e525-e525.
[19] W. Blakemore, Demyelination of the superior cerebellar peduncle in the mouse induced by cuprizone, J. Neurol. Sci. 20 (1) (1973) 63–72.
[20] J.W. Prineas, et al., Multiple sclerosis: pathology of recurrent lesions, Brain 116 (3) (1993) 681–693.
[21] J. Mason, et al., Episodic demyelination and subsequent remyelination within the murine central nervous system: changes in axonal calibre, Neuropathol. Appl. Neurobiol. 27 (1) (2001) 50–58.
[22] V. Murta, F.J. Pitossi, C.C. Ferrari, CNS response to a second pro-inflammatory event depends on whether the primary demyelinating lesion is active or resolved, Brain Behav. Immun. 26 (7) (2012) 1102–1115.
[23] J. Penderis, S.A. Shields, R.J. Franklin, Impaired remyelination and depletion of oligodendrocyte progenitors does not occur following repeated episodes of focal demyelination in the rat central nervous system, Brain 126 (6) (2003) 1382–1391.
[24] A. Taraboletti, et al., Cuprizone intoxication induces cell intrinsic alterations in oligodendrocyte metabolism independent of copper chelation, Biochemistry 56 (10) (2017) 1518–1528.
[25] J.M. Hillis, et al., Cuprizone demyelination induces a unique inflammatory response in the subventricular zone, J. Neuroinflammation 13 (1) (2016) 1–15.
[26] G. El-Akabawy, L.A. Rashed, Beneficial effects of bone marrow-derived mesenchymal stem cell transplantation in a non-immune model of demyelination, Annals of Anatomy-Anatomischer Anzeiger 198 (2015) 11–20.
[27] C. Guglielmetti, et al., Interleukin-13 immune gene therapy prevents CNS inflammation and demyelination via alternative activation of microglia and macrophages, Glia 64 (12) (2016) 2181–2200.
[28] N. Hibbits, et al., Astrogliosis during acute and chronic cuprizone demyelination and implications for remyelination, ASN neuro 4 (6) (2012) AN20120062.
[29] M.K. Sen, et al., The roles of microglia and astrocytes in phagocytosis and myelination: insights from the cuprizone model of multiple sclerosis, Glia 70 (7) (2022) 1215–1250.
[30] R. Aryanpour, et al., 17β-Estradiol reduces demyelination in cuprizone-fed mice by promoting M2 microglia polarity and regulating NLRP3 inflammasome, Neuroscience 463 (2021) 116–127.

[31] M. Mohammadi, et al., Medroxyprogesterone acetate attenuates demyelination, modulating microglia activation, in a cuprizone neurotoxic demyelinating mouse model, Am. J. Neurodegenerative disease 10 (5) (2021) 57.
[32] M. Abdi, et al., Metformin therapy attenuates pro-inflammatory microglia by inhibiting NF-κB in cuprizone demyelinating mouse model of multiple sclerosis, Neurotox. Res. 39 (2021) 1732–1746.
[33] G. Noorzehi, et al., Microglia polarization by methylprednizolone acetate accelerates cuprizone induced demyelination, J. Mol. Histol. 49 (2018) 471–479.
[34] J. Mikita, et al., Altered M1/M2 activation patterns of monocytes in severe relapsing experimental rat model of multiple sclerosis. Amelioration of clinical status by M2 activated monocyte administration, Multiple Sclerosis J. 17 (1) (2011) 2–15.
[35] J. Ślusarczyk, et al., Targeting the NLRP3 inflammasome-related pathways via tianeptine treatment-suppressed microglia polarization to the M1 phenotype in lipopolysaccharide-stimulated cultures, Int. J. Mol. Sci. 19 (7) (2018) 1965.
[36] F. Zhang, et al., Acute hypoxia induced an imbalanced M1/M2 activation of microglia through NF-κB signaling in Alzheimer's disease mice and wild-type littermates, Front. Aging Neurosci. 9 (2017) 282.
[37] J. Lv, et al., MicroRNA let-7c-5p improves neurological outcomes in a murine model of traumatic brain injury by suppressing neuroinflammation and regulating microglial activation, Brain Res. 1685 (2018) 91–104.
[38] H.A. Arnett, et al., Functional genomic analysis of remyelination reveals importance of inflammation in oligodendrocyte regeneration, J. Neurosci. 23 (30) (2003) 9824–9832.
[39] M. Olah, et al., Identification of a microglia phenotype supportive of remyelination, Glia 60 (2) (2012) 306–321.
[40] X. Li, et al., Neural stem cells engineered to express three therapeutic factors mediate recovery from chronic stage CNS autoimmunity, Mol. Ther. 24 (8) (2016) 1456–1469.
[41] S. Lively, et al., Comparing effects of transforming growth factor β1 on microglia from rat and mouse: transcriptional profiles and potassium channels, Front. Cell. Neurosci. 12 (2018) 115.
[42] F. Alexandre, N. Heraud, A. Varray, Is nocturnal desaturation a trigger for neuronal damage in chronic obstructive pulmonary disease? Med. Hypotheses 84 (1) (2015) 25–30.
[43] B.H. Juurlink, The evidence for hypoperfusion as a factor in multiple sclerosis lesion development, Multiple sclerosis Int. 2013 (2013).
[44] C.C. Scholz, et al., Regulation of IL-1β–induced NF-κB by hydroxylases links key hypoxic and inflammatory signaling pathways, Proc. Natl. Acad. Sci. USA 110 (46) (2013) 18490–18495.
[45] R. Yang, J.F. Dunn, Reduced cortical microvascular oxygenation in multiple sclerosis: a blinded, case-controlled study using a novel quantitative near-infrared spectroscopy method, Sci. Rep. 5 (1) (2015) 16477.
[46] D. Paling, et al., Cerebral arterial bolus arrival time is prolonged in multiple sclerosis and associated with disability, J. Cerebr. Blood Flow Metabol. 34 (1) (2014) 34–42.
[47] S.A. Berghoff, et al., Blood-brain barrier hyperpermeability precedes demyelination in the cuprizone model, Acta Neuropathologica Communications 5 (2017) 1–13.
[48] J. Praet, et al., Cellular and molecular neuropathology of the cuprizone mouse model: clinical relevance for multiple sclerosis, Neurosci. Biobehav. Rev. 47 (2014) 485–505.
[49] H. Hong, X.Y. Tian, The role of macrophages in vascular repair and regeneration after ischemic injury, Int. J. Mol. Sci. 21 (17) (2020) 6328.
[50] H.-H. Tsai, et al., Oligodendrocyte precursors migrate along vasculature in the developing nervous system, Science 351 (6271) (2016) 379–384.
[51] D. Zarini, et al., Glial response to intranasal mesenchymal stem cells in intermittent cuprizone model of demyelination, Neurotox. Res. 40 (5) (2022) 1415–1426.
[52] W. Rashid, et al., Abnormalities of cerebral perfusion in multiple sclerosis, J. Neurol. Neurosurg. Psychiatr. 75 (9) (2004) 1288–1293.